# Modeling of Volcanic Clouds for Computer Graphics
# コンピュータグラフィックスのための火山噴煙のモデリング

by

Ryoichi Mizuno
水野 良一

A Master Thesis
修士論文

Submitted to
the Department of Complexity Science and Engineering
on January 31, 2003
in partial fulfilment of the requirements
for the Degree of Master of Frontier Science

Thesis Supervisor: Tomoyuki Nishita　西田 友是
Title: Professor of Complexity Science and Engineering

# ABSTRACT

The modeling of volcanic clouds is useful for natural disaster simulations, entertainments (e.g. games, movies), etc. However, in the field of computer graphics, the modeling of volcanic clouds has almost not been done so far. Then, this thesis proposes two approaches of the modeling of volcanic clouds for computer graphics. One of them uses coupled map lattice (CML) method, which is a kind of cellular automatons for generating patterns. By using the CML method, it becomes possible to simulate the behaviour of the volcanic clouds efficiently. Moreover, to generate desired shaped volcanic clouds, some parameters that allow intuitively control of the volcanic clouds shape are provided. Therefore, by using the proposed method, the realistic behaviour of volcanic clouds can be represented in a practical calculation time. The other approache uses the 2 fluids model (2FM). The 2FM treats two fluids in a scheme, and considers the interaction between the fluids. By using the 2FM, it becomes possible to consider the entrainment, which is essential factor of the dynamics of volcanic clouds. Moreover, the model is simplified based on a plausible assumption and an appropriate approximation. Therefore, by using the proposed method, the quantitatively reasonable three dimensional simulation of volcanic clouds behaviour can be done in a practical calculation time. Moreover, this thesis presents a visualization method of volcanic clouds.

# 論文要旨

コンピュータグラフィックスのための火山噴煙のモデリングは自然災害時のシミュレーションや, 映画・ゲームなどのエンターテイメントに適用でき有用である. しかしコンピュータグラフィックスの分野では, 火山噴煙のモデリングに関する研究はほとんど行われていない. そこで, 本論文は 2 種類のコンピュータグラフィックスのための火山噴煙のモデリング手法を提案する. 一方は, Couppled Map Lattice (CML) 法というパターン生成のためのセルオートマトンの一種を用いる. CML 法を用いることにより, 効率的な噴煙の振舞いのシミュレーションが可能となる. さらに, 提案法では火山噴煙の形状を調整することができるパラメータが提供される. すなわち, 提案法を用いることにより実用的な計算時間で, さまざまな形状の火山噴煙の画像をいくつかのパラメータを変更するだけで生成することができる. 他方は, 2 流体モデル (2FM) を用いる. 2FM を用いることにより, 単一の枠組みにおける 2 つの流体の振舞いのシミュレーションを行うことが可能となる. 提案法では 2FM を用いることにより, 重要な火山噴煙のダイナミクスであるエントレインメントをシミュレートする. さらに, 適切な仮定と近似を用いることによりモデルを簡略化する. すなわち, 提案法を用いることにより実用的な計算時間で, 定量的に根拠のある火山噴煙の画像を生成することができる. さらに, 本論文は火山噴煙の可視化手法を示す.

# Acknowledgement

I would like to thank many people who encouraged and helped me. First, I would like to thank Professor Tomoyuki Nishita (The University of Tokyo) and Assistant Professor Yoshinori Dobashi (Hokkaido University) for their numerous useful advice and discussion. I am also grateful to Assistant Professor Takehiro Koyaguchi (The University of Tokyo) and Mr. Yujiro Suzuki (The University of Tokyo) for giving me valuable suggestions about the dynamics of volcanic clouds. Moreover, I would like to thank to Dr. Yoshinori Mochizuki (ExpressionTools, Inc.), Mr. Robin Bing-Yu Chen (The University of Tokyo), Mr. Kei Iwasaki (The University of Tokyo), Mr. Toshiyuki Haga (NTT DATA Corp.), and Mr. Ryo Miyazaki (The University of Tokyo) for teaching me many know-how of the computer graphics. Furthermore, I would like to appreciate to Mr. Manabu Ishii (Tokyo Metropolitan Institute of Technology), Mr. Tomoharu Iwata (The University of Tokyo), Ms. Ayako Onzo (Tokyo Institute of Technology), Mr. Keisuke Suzuki (The University of Tokyo), Mr. Ryuta Suzuki (Toin University of Yokohama), and Mr. Youhei Wakayama (Meiji Pharmaceutical University) for their comment and interrogatories. Finally, I would like to thank all the members of Nishita laboratory of The University of Toyko. In particular, I extend gratitude to Mr. Yosuke Bando, Mr. Namba Ryuichi, Mr. Nobuo Yasuhara, Mr. Tetsuichi Yanagida, and Mr. Kenichi Amou who encouraged and helped me for these two years. I cannot complete this thesis without their help.

# List of Figures

# Contents

# Chapter 1

# Introduction

The modeling of volcanic clouds is useful for natural disaster simulations, entertainments (e.g. games, movies), etc. However, there are not many researches on the modeling of volcanic clouds. Especially, in the field of computer graphics, that kinds of researches have almost not been done so far. Although there are several commercial modeling products that can generate volcanic clouds images [53], they can only obtain the motion of the volcanic clouds according to the orbits of some particles which are set by professional users. On the other hand, the model of volcanic clouds for computer graphics is frequently demanded by industrial world [27].

In the field of computer graphics, the model of volcanic clouds should satisfy the following requirements at least.

- The model can represent visually plausible and beautiful volcanic clouds.
- The simulation using the model can be done in a practical calculation time.

Additionally, the model of volcanic clouds for computer graphics should satisfy at least one of the following requirements.

- The model can represent the volcanic clouds that are desired by user with only easy operations, i.e., the system does not need the user's expertise of the dynamics of volcanic clouds. This kind of models could be used for entertainments.

- The model is designed based on the dynamics of volcanic clouds. This allows user to use physically meaningful parameters to generate volcanic clouds. Viz, the user can obtain the quantitatively correct result. This kind of models could be used for natural disaster simulations.

In this thesis, two approaches of the modeling of volcanic clouds for computer graphics are proposed. One of the approaches is the modeling method of volcanic clouds using the coupled map lattice (CML) method [27, 28, 29]. The CML method [19, 20, 47, 48, 49, 50, 51] is a kind of cell dynamics, which generates patterns (see [50] for the details). The important advantages of using the CML method are that it is easy to implement and low computational cost. The aims of this approach are as follows.

- The realistic behaviour of volcanic clouds can be represented in a practical calculation time.

- The various shapes of volcanic clouds can be generated by changing only several parameters.

To achieve the practical calculation of the behaviour, the CML method is introduced as the solver of the Navier-Stokes equations, which describe the time evolution of fluid. Moreover, to generate desired shaped volcanic clouds, some parameters that allow intuitively control of the volcanic clouds shape are provided by the proposed method. Chapter 3 describes the details of this approach.

The other approach is the modeling method of volcanic clouds using "2 fluids model" [30]. Here, the 2 fluids model (2FM) treats two fluids in a scheme, and considers the interaction between the fluids. The aims of this approach are as follows.

- The realistic and quantitatively reasonable behaviour of volcanic clouds can be represented as the result of the simulation based on the simplified dynamics of volcanic clouds.

- The quantitatively reasonable three dimensional simulation of volcanic clouds behaviour can be done in a practical calculation time.

To represent the realistic and quantitatively reasonable behaviour of volcanic clouds, the dynamics of volcanic clouds should be considered. Especially, the nonlinear relationship between the volcanic cloud density and the mass fraction of the magma (or the air) is one of the essential factors of the dynamics. Hence, the nonlinear relationship is considered in the proposed method. However, it is hard to simulate the behaviour of volcanic clouds in a three dimensional analysis space in a practical calculation time with the consideration of the nonlinear relationship. To overcome the difficulty, the model is simplified based on a plausible assumption and an appropriate approximation. The details of this approach is described in Chapter 4.

The fast and stable fluid solver proposed by Fedkiw *et al.* [9] is basically used for the solution of both of the proposed models. By using a technique called the semi-Lagarngian advection scheme [37], the solver can calculate the Navier-Stokes equations stably even if the time step is large. Moreover, the solver can represent small scale vortexes lost during the numerical calculation process by using a technique called the vorticity confinement [38].

The visualization of the calculation results of the modeling part is indispensable for almost all of researches in the computer graphics field. Note that the visualization in the computer graphics field often has different meaning than the visualization in the other fields. That is, in the computer graphics field, the visualization mainly does not mean show some graphs that show the numerical profiles of the results, but mostly means show realistically visible objects that are led by the results, and is often called "rendering". In this thesis, the visualization means the rendering normally. In the computer graphics field, the researches that treat natural phenomena should visualize the simulation results to show what the researches got. The calculation results of the behaviour of volcanic clouds provided by the proposed methods are visualized using the extended version of the splatting algorithm using the billboards [1, 25, 42]. By using this visualization method [5], the clouds together with the atmospheric scattering can be visualized. Therefore, the results of the visualization are photo-realistic. The basic idea for applying the method to the visualization of volcanic clouds is described in Chapter

5.

The next chapter discusses the related works, and finally Chapter 6 concludes and discusses future research.

# Chapter 2

# Related Work

This thesis could be divided into two horn categories, which are the modeling and the visualization. Then, the related works are discussed separately with respect to the categorization.

## 2.1 Related Work of the Modeling of Volcanic Clouds

### 2.1.1 Related work in the computer graphics field

As described in Chapter 1, although there is almost no research on the modeling of volcanic clouds in the field of computer graphics, but there are many researches on the modeling of the complex behaviour of fluids such as smoke [9, 11, 37], cloud [4, 5, 17, 26], water [8, 10, 12], flame [22, 32, 52], etc. The researches deeply related the proposed methods are discussed in the following. Kajiya and Herzen proposed a simulation method for cloud by solving the Navier-Stokes equations [17]. However, at that time (1984), they could only calculate on few voxels due to the lack of the calculation ability of computer. Therefore their method could not represent the realistic cloud (see Figure 2.1). Foster and Metaxas proposed a method that can generate realistic motion of turbulent smoke on relatively few voxels [11] (see Figure 2.2). However, this method is stable only when the time step is very small and costs a lot of time for calculation. Stam introduced the semi-Lagrangian advection scheme to calculate the advection term of the Navier-Stokes equations [37]. By using the semi-Lagrangian advection scheme, it is possible to calculate the advection term of the Navier-Stokes equations stably even if the time step is large (see Figure 2.3). Although in the field of computational fluid dynamics, the semi-Lagrangian advection scheme had already been used in those days, it was the first trial of the introduction of the scheme to the computer graphics field. The advection term makes the Navier-Stokes equations nonlinear, and is prime factor of the constraint of the time step. That is, when the time step is large, the calculation of the Navier-Stokes equations using any previous fluid solvers for computer graphics at that time is unstable. Fedkiw *et al.* provided a technique called the vorticity confinement which is applied to Stam's model [9]. The vorticity confinement can represent small-scale vortexes lost during the numerical calculation process [38]. However, the methods provided by Stam and Fedkiw *et al.* premised for a small space such as inside a room or just a small area. Therefore, their methods cannot take some factors, which are related to height, like the variation of the atmospheric density with respect to height into consideration. Miyazaki *et al.* proposed a simulation method for cloud behaviour by using the CML method [26]. The CML method was originally developed by Kaneko, and is an extended method of cellular automaton [19]. The advantages of the CML method are that it is easy to implement and the computational cost is small. Yanagita and Kaneko proposed a method for the modeling and characterization of the clouds dynamics using the CML method [51]. Miyazaki *et al.* extended their works, and applied to the modeling of clouds for computer graphics. Their method can generate realistic clouds in a practical calculation time (see Figure 2.5). However, the method provided by Miyazaki *et al.* was designed to generate the animations of clouds, and cannot be applied to volcanic clouds directly.

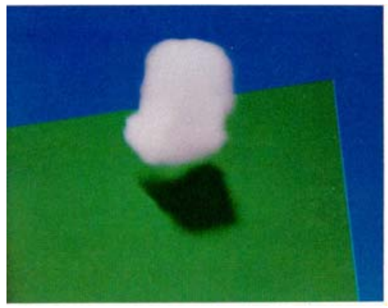

Figure 2.1: Cumulus clouds generated by the method of Kajiya [17]. The simulation was done on $10 \times 10 \times 20$ voxels. The time for the simulation per a time step was around 10 seconds. The computation was done on a VAX 11/780.

Figure 2.2: Smoke rising from a chimney on a hot day generated by the method of Foster and Metaxas [11]. The simulation was done on $60 \times 60 \times 45$ voxels. The computation was done on an SGI Indigo 2.

Figure 2.3: Gas generated by the method of Stam [37]. The number of voxel ranged from $10^3$ to $30^3$, with frame rates fast enough to monitor the animations while being able to control their behaviour. The computation was done on an SGI Octane with a R10K processor.

Figure 2.4: Rising smoke generated by the method of Fedkiw *et al.* [9]. Notice how the vorticies are preserved in the smoke. The simulation time for $100 \times 100 \times 40$ voxels was roughly 30 seconds/time step. The computation was done on a dual Pentium III 800MHz CPU machine.

Figure 2.5: Cumulus clouds generated by the method of Miyazaki *et al.* [26]. The simulation was done on $178 \times 178 \times 44$ voxels. The calculation time for the simulation was few seconds/time step. The computation was done on a Pentium III 1GHz CPU machine.

### 2.1.2 Related work in the other fields

In the other fields, there are a number of researches of the volcanic clouds dynamics and the modeling volcanic clouds. The large majority of such kinds of researches have been done in the field of earth and planetary sciences. One of the significant researches of the analysis and modeling of volcanic clouds dynamics is the research of Woods [43]. He analyzed the dynamics of the vertical structure of volcanic clouds, and proposed the one dimensional model of volcanic clouds. Then, Woods' model was followed by some researchers, for example, Dobran and Neri [6], Woods and Bower [44], and Neri and Macedonio [31]. However, the models are one dimensional. Thus, although their works are important, it is impossible to apply them to the visualization directly. Valentine and Wohletz proposed the axisymmetric two dimensional model of volcanic clouds [41]. Moreover, the model of Valentine and Wohletz was followed by Ishimine and Koyaguchi [15], Ishimine [16], and Susuki [39]. From the point of view of the computer graphics, their works made a great progress since they made it possible to visualize the shapes of volcanic clouds. However, the models are still axisymmetric two dimensional. Therefore, their models cannot be directly applied to the visualization of volcanic clouds for computer graphics. Suzuki suggested that Suzuki's model can be extend to the three dimensional model [39]. But, the computational cost of the simulation in a three dimensional analysis space using the model is too expensive to applicate it for the computer graphics purpose. In fact, several days are needed to generate the visually plausible volcanic clouds with a current high-end computer.

### 2.1.3 Features of the proposed modeling methods

The proposed modeling method that uses the CML method can represent the three dimensional realistic behaviour of volcanic clouds in a practical calculation time, and can generate the various shapes of volcanic clouds by changing only several parameters. The other proposed modeling method using the 2FD can represent the three dimensional, realistic and quantitatively reasonable behaviour of volcanic clouds in a practical calculation time.

## 2.2 Related Work of the Visualization of Clouds

The simulation results of the behaviour of volcanic clouds provided by the proposed models are visualized using the method of clouds proposed by Dobashi *et al.* that considers single scattering effect [5] (See Figure 2.6). Originally, this method was the visualization method of lightning considering scattering effects due to clouds and atmospheric particles. In this thesis, this method is applied to the visualization of volcanic clouds.

One of the simplest way to visualize clouds is to use the mapping techniques, such as the method developed by Gardner [13] (see Figure 2.7). However, these methods cannot take into account scattering due to particles. Therefore, that kind of methods are not suitable for the photo-realistic visualization of natural phenomena. To achieve the photo-realistic visualization, the considering of scattering is necessary. Many such methods have been proposed [3, 7, 17, 18, 24, 33, 34, 35, 36, 37]. Some of them can take into account multiple scattering [17, 24, 33, 36]. Nishita *et al.* took into account the effect of skylight on clouds' color [33] (see Figure 2.8). However, although the considering of the effects of multiple scattering and skylight is important for the photo-realistic visualization, it is time-consuming. So, in the visualization method of the results generated by the proposed models, the effects of multiple scattering are approximated as constant ambient light. Note that this method takes into account the single scattering effect due to the presence of clouds and atmospheric particles. Recently, hardware-accelerated visualization methods of the volume density that is similarly to clouds have been proposed. One of the most popular the methods is to use the three dimensional textures. The idea of the three dimensional textures was first suggested by Max *et al.* [23]. The three dimensional texture technique predefines texture values to any points on the surface of the visualized object. Thus, the technique is analogous to carving a statue from a block of material [2]. Stam used the three dimensional textures with utilizing of graphics hardware to visualize gas fast [37] (see Figure 2.3). However, the three dimensional texture mapping is still expensive and not universally available as are two dimensional textures. The visualization method of the results generated by the proposed models can provided photo-realistic image on a current standard personal computer in a practical calculation time. That is, the visualization method uses two dimensional textures. Thus, this method can do fast calculation of the scattering by utilizing graphics hardware.

Figure 2.6: Flash of lightning in clouds generated by the method of Dobashi *et al.* [5]. The computational time was less than 0.5 seconds. The computation was done on a Pentium III 730 MHz CPU machine with NVIDIA GeForce2GTS machine.

Figure 2.7: Landscape using combine two dimensional and three dimensional clouds model generated by the method of Gardner. [13]. The computational time was 20 minutes. The computation was done on a Data Eclipse 2/250.

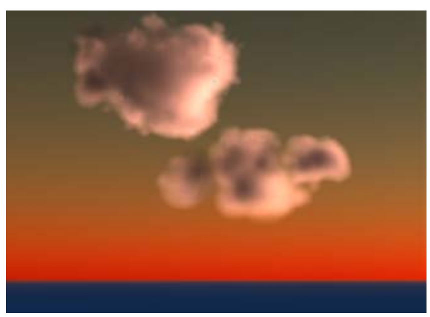

Figure 2.8: Clouds in the sky at dawn generated by the method of Nishita *et al.* [33]. This image depict beautiful variations in the color of clouds and sky due to multi-scattering. The computational time was 20 minutes. The computation was done on an IRIS Indigo2 (R4400).

# Chapter 3

# Modeling of Volcanic Clouds using CML

## 3.1 Introduction

In this chapter, the model of volcanic clouds using the CML method [27, 28, 29] is proposed. In this model, the Navier-Stokes equations are used, and the equations are solved by using the CML method that can be applied as an efficient fluid solver [19, 20, 47, 48, 49, 50, 51] (see [50] for the details). Moreover, a stable solving method for proposed model is presented that is to use the semi-Lagrangian advection scheme [37], which is a stable method even if the time step is large. Hence, in this system, the behaviour of the volcanic clouds can be calculated in a practical calculation time, and various shapes of the volcanic clouds can be generated by only changing some parameters. Therefore, photo-realistic images of various shapes of volcanic clouds can be created by the proposed approach efficiently.

There are many factors that decide the shape of the volcanic clouds. In these factors, the eruption magnitude, the buoyancy, the decreasing of the volcanic cloud density, and the temperatures of the magma and the volcanic clouds are important. Since the ascending current due to the temperature of the magma can be considered as the eruption velocity, and the buoyancy due to the temperature of the volcanic clouds can be considered as the buoyancy generated by the difference between the volcanic cloud density and the atmospheric density, the temperatures of the magma and the volcanic clouds can be simplified to enhance the simulation speed. Therefore, the proposed model is designed by taking the following important factors that decide the shape of the volcanic clouds.

**Eruption magnitude** The eruption magnitude is decided by the eruption velocity of volcanic clouds and the initial volcanic cloud density, and it decides the scale of the volcanic clouds.

**Buoyancy** The buoyancy is generated by the difference between the volcanic cloud density and the atmospheric density. The conic shaped clouds are generated due to the buoyancy.

**Decreasing of the volcanic cloud density** The volcanic cloud density can be decreased due to the loss of the pyroclasts. The diversities of the volcanic clouds shapes due to the differences of the contents inside the volcanic clouds are decided by the distribution varieties of the loss of the pyroclasts.

## 3.2 Model

### 3.2.1 Evolution of velocity field

The atmospheric fluid and the volcanic clouds has small viscosity, and the eruption velocity of the volcanic clouds is less than the sonic speed. Therefore, it is assumable that the following non-viscosity Naivier-Stokes equations can be used to describe the time evolution of the velocity field.

$$\nabla \cdot \mathbf{u} = 0, \tag{3.1}$$

$$\frac{\partial \mathbf{u}}{\partial t} = -(\mathbf{u} \cdot \nabla)\mathbf{u} - \nabla p + \mathbf{f}, \tag{3.2}$$

where $\mathbf{u}$ is a velocity vector, $p$ is the pressure, and $\mathbf{f}$ is an external force that is applied to the velocity field. Equation (3.1) means that the inflow and the outflow of a unit cell are balanced, and is called the "continuity equation". This equation is the constraint, which projects the velocity vector to the divergent free field. The first term of the right hand of Equation (3.2) means the advection of the velocity vector, and is called the "advection term". The second term means the variation of the velocity caused by the gradient of the pressure, and is called the "pressure term". The third term means that the velocity is varied by the external force, and is called the "external force term". In the proposed method, Equation (3.1) and the pressure term of Equation (3.2) are approximated by using the method of CML (see [50] for the details). Therefore, the following approximated Navier-Stokes equation can be obtained.

$$\frac{\partial \mathbf{u}}{\partial t} = -(\mathbf{u} \cdot \nabla)\mathbf{u} + \eta \nabla(\nabla \cdot \mathbf{u}) + \mathbf{f}, \tag{3.3}$$

where $\eta$ is a positive constant which means the rate of diffusion, and is called the "diffusion coefficient". Factually, the diffusion coefficient controls the scales of the vortexes. The approximated Navier-Stokes equation does not need iterative calculation to solve the continuity and the pressure effect, although iterative calculation is generally needed to solve the Poisson equation to consider the continuity and the pressure effect in other methods.

### 3.2.2 Evolution of volcanic clouds

The volcanic clouds are transported by the atmospheric fluid, and the volcanic cloud density is decreased due to the loss of the pyroclasts. Therefore, the following equation for volcanic cloud density $\rho$ can be defined.

$$\frac{\partial \rho}{\partial t} = -(\mathbf{u} \cdot \nabla)\rho - \kappa(z)\rho, \tag{3.4}$$

where $\kappa(z)$ is a function of height $z$ and means the decreasing rate of $\rho$. In this thesis, $\kappa(z)$ is called as the "decreasing rate", and it should be set with the following two features.

- Near the vent, the volcanic clouds include many large pyroclasts called the "volcanic blocks". Therefore, $\rho$ decreases rapidly due to the fall of the volcanic blocks. To simulate this phenomenon, $\kappa(z)$ needs to be set large in this region.

- In higher region, the volcanic clouds consist of many small pyroclasts called the "volcanic ash" and air, and then the pyroclasts are hardly lost. Therefore, $\kappa(z)$ needs to be set small in this region.

The diversity of the volcanic clouds shapes due to the differences of the constituents of the volcanic clouds can be represented by setting the decreasing rate $\kappa(z)$.

### 3.2.3 Buoyancy

Due to the difference between the volcanic cloud density and the atmospheric density, the buoyancy is occurred, which affects the velocity field. The buoyancy $\mathbf{f}_{buoy}$ is defined as Equation (3.5). Note when the perpendicular component of $\mathbf{f}_{buoy}$ is a negative, the buoyancy works perpendicularly downward. That is, $\mathbf{f}_{buoy}$ works as the gravity.

$$\mathbf{f}_{buoy} = \alpha(\rho_{atm}(z) - \rho)\mathbf{z}, \tag{3.5}$$

where $\alpha$ is a positive constant which controls the strength of the buoyancy, $\mathbf{z}$ is a perpendicularly upward unit vector, and $\rho_{atm}(z)$ is the atmospheric density, which is defined as an exponential function of height as the following equation.

$$\rho_{atm}(z) = \rho_0 \exp\left(-\frac{z}{H_e}\right), \tag{3.6}$$

where $\rho_0$ is the atmospheric density at the ground ($z = 0$), and $H_e$ is the degree of the atmospheric density variety with respect to height, and called the "scale height". The buoyancy plays an important role to decide the shape of the volcanic clouds, and the following dynamics generates the conic shaped clouds.

- In the region which height is low called the "gas thrust region", the atmospheric density is less than the volcanic cloud density. Thus, the perpendicular component of $\mathbf{f}_{buoy}$ becomes a negative, and the buoyancy works perpendicularly downward. However, the momentum of the eruption is more dominant than the buoyancy. Therefore, the volcanic clouds are delivered toward upward.

- In the higher region called the "convective region", the atmospheric density is larger than the volcanic cloud density. Thus, the perpendicular component of $\mathbf{f}_{buoy}$ becomes a positive, and the buoyancy works perpendicularly upward. Hence, the volcanic clouds are delivered toward upward.

- In the region higher than the convective region called the "umbrella region", the atmospheric density and the volcanic cloud density are almost balanced. Therefore, $\mathbf{f}_{buoy}$ becomes almost $\mathbf{0}$, and the volcanic clouds are not delivered perpendicularly no longer.

The proposed approach can generate realistic volcanic clouds behaviour by satisfying these dynamics.

### 3.2.4 Fluid solver

The fluid solver for the model using the CML method is described in this subsection.

#### Setting of analysis space

The analysis space is represented as $n_x \times n_y \times n_z$ voxels. Each voxel is a cube with uniform size. The velocity vector $\mathbf{u}$ and the volcanic cloud density $\rho$ are defined as the state variables at the center of each voxel. As the initial state, $\mathbf{u}$ is set to be a small value by using a random function, and $\rho$ is set to be zero. But, for the voxels located to the mountain (the shaded squares in Figure 3.1), $\mathbf{u}$ is set to be a zero vector.

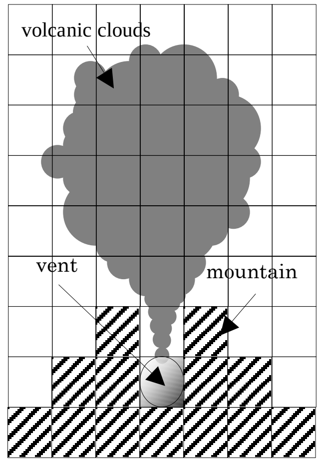


Figure 3.1: Outline of the analysis space.

Then, the decreasing rate $\kappa(z)$ and the strength of the side wind $\mathbf{f}_{wind}(z)$ at each height can be defined through the graphical user interface (GUI) shown in Figure 3.2, and the atmospheric density at each height $\rho_{atm}(z)$ is defined by Equation (3.5).

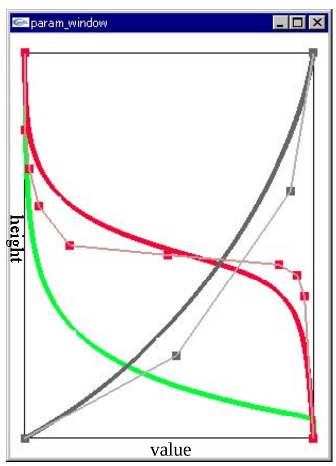


Figure 3.2: The GUI for setting the functions of height. The red curve denotes $\kappa(z)$, the gray curve denotes $\mathbf{f}_{wind}(z)$, and the green curve denotes $\rho_{atm}(z)$. The horizontal axis is the value of each function, and the vertical axis is height $z$. Each value is standardized by its maximum to show in the GUI.

As shown in Figure 3.2, the decreasing rate $\kappa(z)$ and the strength of the side wind $\mathbf{f}_{wind}(z)$ can be set by dragging the corresponding control points of the Bézier curves. Moreover, the atmospheric density $\rho_{atm}(z)$ defined by Equation (3.5) is shown. Finally, the eruption velocity $\mathbf{u}_{src}$ and the initial volcanic cloud density $\rho_{src}$ that decide the eruption magnitude are assigned to the voxels correspond to the vent (the circle in Figure 3.1). It is also possible to make the volcanic clouds erupt with a spread. In the proposed method, the diversity of volcanic clouds shapes can be represented by only changing these parameters.

**Sequential solver**

The time evolution of the volcanic clouds behaviour can be obtained by iterating the following sequential processes.

1. **Add force**
   "Add force" is the process to add the external force to the velocity fluid.

2. **Advect**
   "Advect" is the process to advect the state variables.

3. **Pattern**
   "Pattern" is the process to generate the vortex patterns using the CML method.

4. **Decrease**
   "Decrease" is the process to decrease the volcanic cloud density with respect to the loss of the pyroclasts.

**Add force** In Add force process, the effect of the external force as the third term of the right hand of Equation (3.3) is calculated. In this method, the external force $\mathbf{f}$ is the sum of the buoyancy $\mathbf{f}_{buoy}$, and the strength of the side wind $\mathbf{f}_{wind}(z)$. Hence, the equation for updating the velocity vector $\mathbf{u}$ is expressed as follows.

$$\mathbf{u}^* = \mathbf{u} + (\mathbf{f}_{buoy} + \mathbf{f}_{wind}(z))\Delta t, \tag{3.7}$$

where $\mathbf{u}^*$ is the velocity vector after being updated while a time step $\Delta t$, respectively.

**Advect** In Advect process, the effects of the advection as the first term of the right hand of Equation (3.3) and the first term of the right hand of Equation (3.4) are calculated. For this calculation, the semi-Lagrangian advection scheme is used. As illustrated in Figure 3.3, a path $\mathbf{p}(\mathbf{x}, s)$ is defined as a parametric function of time parameter $s$ by tracing a particle, which is located position $\mathbf{x}$ to backward along the velocity field at time $t$. Thus, $\mathbf{p}(\mathbf{x}, s)$ represents a position that the particle existed at time $(t - s)$. The state variables at position $\mathbf{x}$ at time $t$ are advected from position $\mathbf{p}(\mathbf{x}, \Delta t)$. Hence, the equations for updating the state variables are expressed as follows.

$$\mathbf{u}^*(\mathbf{x}) = \mathbf{u}(\mathbf{p}(\mathbf{x}, \Delta t)), \tag{3.8}$$

$$\rho^*(\mathbf{x}) = \rho(\mathbf{p}(\mathbf{x}, \Delta t)), \tag{3.9}$$

where $\mathbf{u}^*$ and $\rho^*$ are the velocity vector and the volcanic cloud density after being updated while a time step $\Delta t$ respectively.

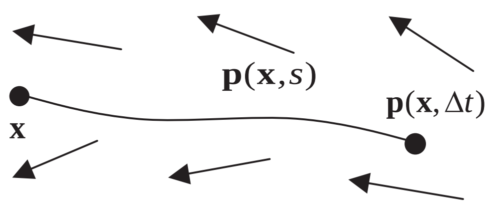


Figure 3.3: Path setting in the semi-Lagrangian advection scheme.

**Pattern** In Pattern process, the effect of the generating of the vortex patterns as the second term of the right hand of Equation (3.3) is calculated. The equation for updating the velocity vector $\mathbf{u}$ is expressed as follows.

$$\mathbf{u}^* = \mathbf{u} + \eta \nabla(\nabla \cdot \mathbf{u}) \Delta t, \tag{3.10}$$

where $\mathbf{u}^*$ is the velocity vector after being updated while a time step $\Delta t$. A discrete version of Equation (3.10) is shown in Equation (3.11). Here, only the equation for updating $u_{i,j,k}$, which is the $u$ component of the velocity vector $\mathbf{u}$ ($\equiv (u, v, w)$) of voxel $(i, j, k)$ is described.

$$\begin{aligned} u^*_{i,j,k} &= u_{i,j,k} + \eta\{(u_{i+1,j,k} + u_{i-1,j,k} - 2u_{i,j,k})/2 \\ &+ (v_{i+1,j+1,k} - v_{i+1,j-1,k} - v_{i-1,j+1,k} + v_{i-1,j-1,k} \\ &+ w_{i+1,j,k+1} - w_{i+1,j,k-1} - w_{i-1,j,k+1} + w_{i-1,j,k-1})/4\}\Delta t, \end{aligned} \tag{3.11}$$

where $u^*_{i,j,k}$ is the $u$ component of the velocity vector after being updated while a time step $\Delta t$. The updating of the $v$ and $w$ components can be expressed in the same way.

**Decrease** In Decrease process, the decrease of the volcanic cloud density as the second term of the right hand of Equation (3.3) is calculated. The equation for updating the volcanic cloud density $\rho$ is expressed as follows.

$$\rho^* = \rho - \kappa(z)\rho\Delta t, \tag{3.12}$$

where $\rho^*$ is the volcanic cloud density after being updated while a time step $\Delta t$.

## 3.3 Result

The images generated by the proposed method are shown in Figures 3.4-3.8. Figures 3.4-3.7 show the volcanic clouds when there is no side wind. Figures 3.4, 3.5 and 3.8 also show the profiles of the function of height. Figure 3.4 is the image to show the case when the decreasing rate in the gas thrust region is set to be relatively large, so that the volcanic clouds include many large pyroclasts. Conic volcanic clouds were generated as the result. Figure 3.5 shows the case when the decreasing rate in the gas thrust region is set to be relatively small, hence the volcanic clouds consist small pyroclasts and air. Spread volcanic clouds were generated as the result. Figure 3.6 shows the case when the eruption velocity and the initial volcanic cloud density are relatively large, so that the eruption magnitude is relatively large. Narrow and high volcanic clouds were generated as the result. Figure

3.7 shows the case when the eruption velocity and the initial volcanic cloud density are relatively small, so that the eruption magnitude is relatively small. Round and low volcanic clouds were generated as the result. Besides the eruption velocity and the initial volcanic cloud density, the parameters in Figures 3.6 and 3.7 are set as those in Figure 3.4. Figure 3.8 shows a sequence of images of an animation of the volcanic clouds affected by the side wind. The parameters except the strength of the side wind are set as those in Figure 3.4. Figure 3.9 shows photographs of real volcanic clouds and the volcanic clouds generated by the proposed method for comparison. Unfortunately, only grayscale photographs were available. Hence, the images are shown in grayscale to compare equally. However, they seem enough for the comparison of the shapes of volcanic clouds. Figure 3.9a is a photograph of conic shaped volcanic clouds, and Figure 3.9b is a photograph of the round and low volcanic clouds. The shapes of clouds' outline of the photographs are similar to the images generated by the proposed method.

All of the images are visualized as the simulation results on $100\times100\times100$ voxels, by using the visualization method described in Chapter 5. The computational time of the simulation was approximately 1 second per time step on a Pentium 4 2.8 GHz CPU machine, and the computational time for the simulation almost proportion to the number of voxels. When the CML method is unused, several times simulation time is required at least. It depends on a choice of the Poisson solver.

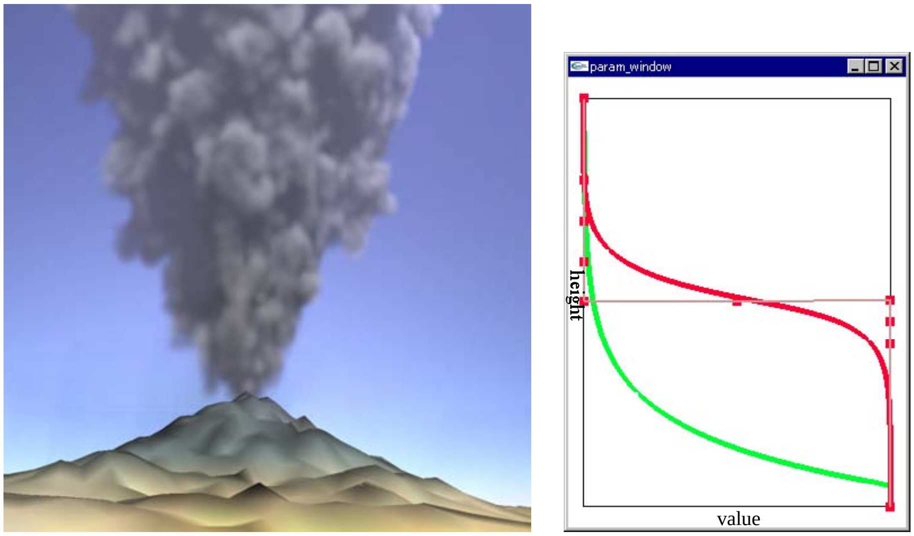


Figure 3.4: Conic volcanic clouds generated by the proposed method. In the graph, the red curve denotes $\kappa(z)$, and the green curve denotes $\rho_{atm}(z)$. The horizontal axis is the value of each function, and the vertical axis is height $z$. $\kappa(z)$ when $z$ is small was set relatively large.

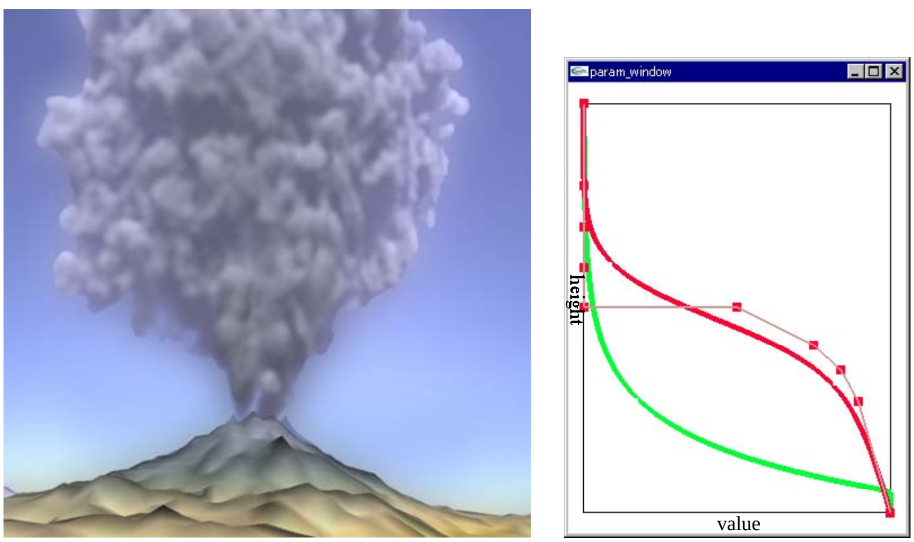


Figure 3.5: Spread volcanic clouds generated by the proposed method. $\kappa(z)$ when $z$ is small was set relatively small.

Figure 3.6: Narrow and high volcanic clouds generated by the proposed method. The eruption velocity and the initial volcanic cloud density were relatively large.

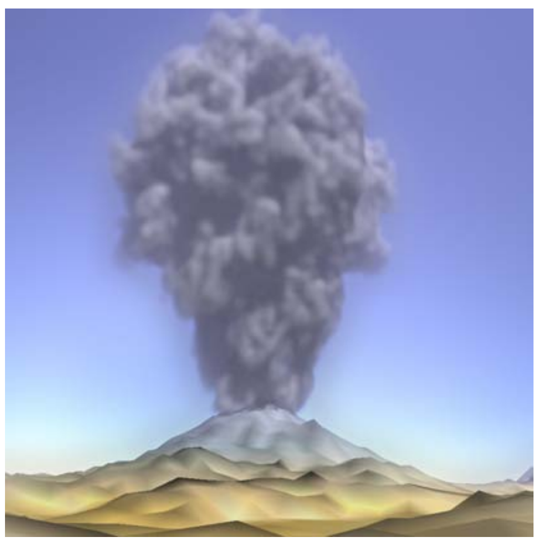

Figure 3.7: Round and low volcanic clouds generated by the proposed method. The eruption velocity and the initial volcanic cloud density were relatively small.

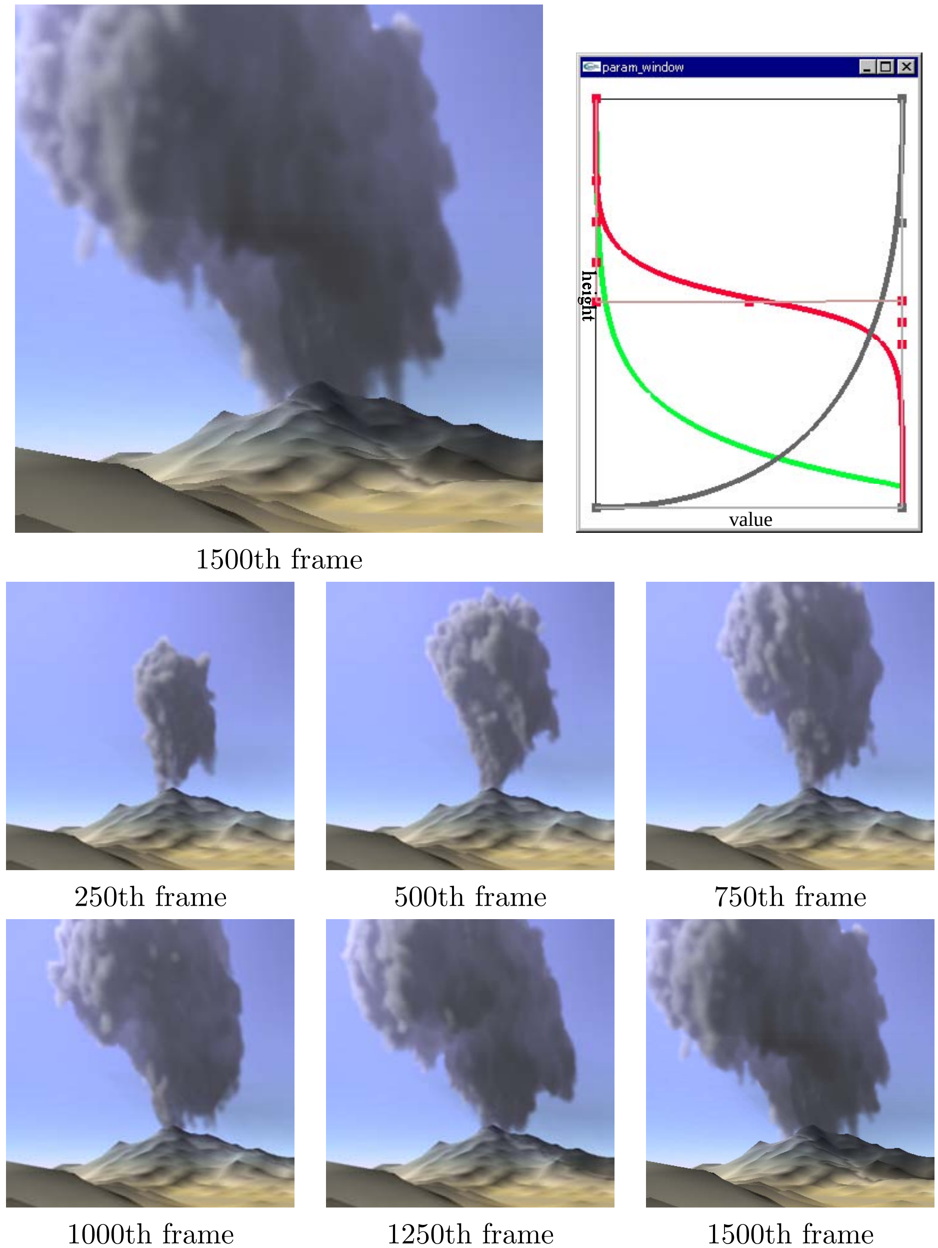


Figure 3.8: A sequence of images of an animation of the volcanic clouds affected by the side wind generated by the proposed method. In the graph, the gray curve denotes $\mathbf{f}_{wind}(z)$.

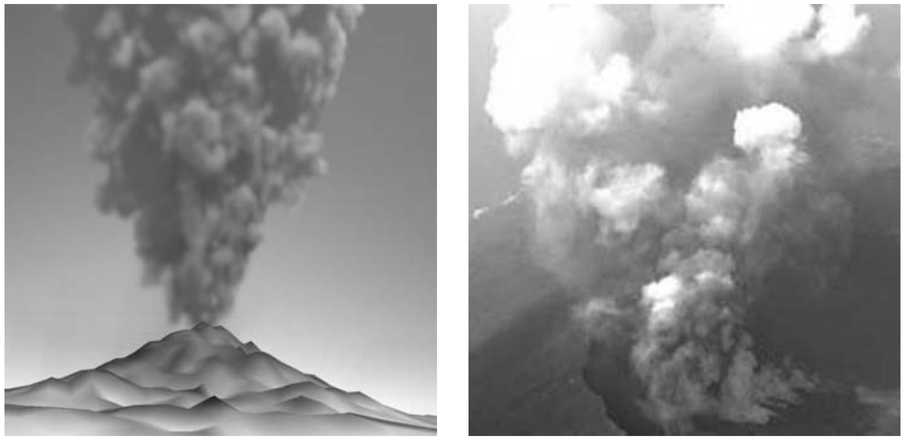

(a)

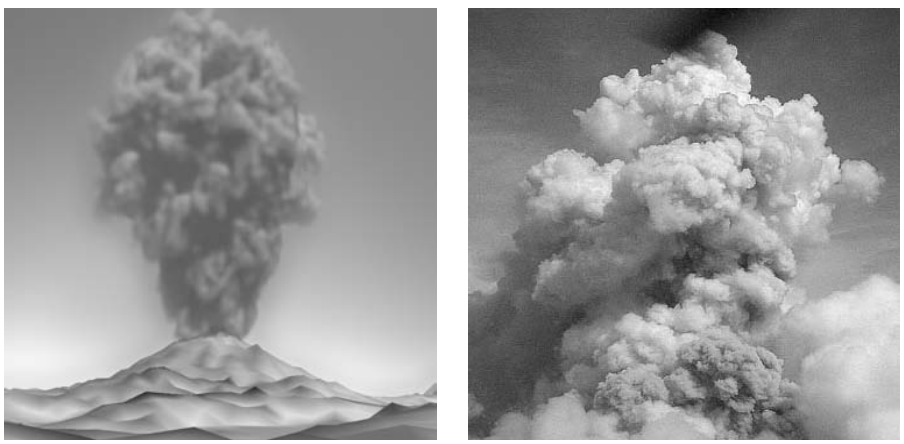

(b)

Figure 3.9: Photographs of real volcanic clouds and the volcanic clouds generated by the proposed method for comparison. (a) is for compare with Figure 3.4, and (b) is for compare with Figure 3.7. The copyrights of the photographs have been reserved by Prof. Setsuya Nakada.

## 3.4 Conclusion and Future Work

In this chaper, a method for the modeling of volcanic clouds using the CML method was provided. The major features of the proposed method are:

- The realistic behaviour of volcanic clouds is represented by considering the eruption magnitude decided by the eruption velocity and the initial volcanic cloud density, the buoyancy generated by the difference between the volcanic cloud density and the atmospheric density, and the decreasing of the volcanic cloud density due to the loss of the pyroclasts.
- Various shapes of volcanic clouds can be generated by only changing some parameters.
- An efficient simulation is achieved by using the CML method.

To enhance the calculation speed of the simulation, it is a good idea to implement the proposed model by using graphics hardware. Harris *et al.* proposed a fast calculation method of the CML using graphics hardware [14], although graphics hardware is generally used for rendering. Implementation of the CML part of the proposed model using graphics hardware will be a part of the future work.

# Chapter 4

# Modeling of Volcanic Clouds using 2FM

## 4.1 Introduction

In this chapter, the model of volcanic clouds using the 2FM [30] is proposed. The prime aim of this approach is to represent realistic and quantitatively reasonable behaviour of volcanic clouds in a practical calculation time. To achieve only the representation of the quantitatively reasonable behaviour, it might be suitable to use the model proposed by Suzuki [39]. However, to achieve the practical calculation of the behaviour, it seems that the model is too complex (see Subsection 2.1.2 for the details). That is, a simplified model is required. Therefore, the proposed model takes one of the most important dynamics of volcanic clouds, which is the nonlinear relation between the volcanic cloud density and the mass fraction of the magma/air. Here, let us clarify the definitions of the volcanic clouds and the magma. Though the magma may be regarded as red heated and very sticky fluid in general, in this thesis, the magma is defined as the mixture of the volcanic gas and the pyroclasts. Then, the volcanic clouds are defined as the mixture of the magma and the air. When the eruption is explosive, the pyroclasts in the magma are disintegrated due to the momentum of the eruption, and their grain size becomes several millimeters. Hence, the pyroclasts and the volcanic gas reach to the thermal equilibrium. Moreover, the relative velocity between the pyroclasts and the volcanic gas is negligible. Hence, the magma can be treat as one fluid. Therefore, the volcanic clouds are consisted of two fluids, which are the magma and the air. Consequently, the behaviour of the volcanic clouds is modeled using the 2FM, which can treat two fluids in a scheme. Moreover, by appropriate approximation and assumption, the look-up table that expresses the nonlinear relation between the density of the volcanic clouds, and the mixing rate of the magma and the air is made to enhance efficiency of the proposed model. By using this model, the modeling of volcanic clouds with an explosive eruption based on its simplified dynamics is achieved in a practical calculation time.

## 4.2 Dynamics of entrainment

The magma is erupted from the vent as a turbulent flow. Just behind the eruption, the density of the magma is several times of the surrounding air. Therefore, the velocity of the volcanic clouds that are almost the magma slows down rapidly. However, at the same time, the volcanic clouds entrain the surrounding air. In this thesis, the entrainment of the surrounding air is simply called "entrainment". This goes also in the field of earth and planetary sciences. The entrained air is heated instantaneously by the heat of the magma, and the volcanic clouds expand. Then, the density of the volcanic clouds decrease promptly due to the expansion. Consequently, the volcanic cloud density becomes less than the ambient atmospheric density. As the result, the buoyancy is occurred, and the volcanic clouds are delivered toward upward. Since the atmospheric density decreases with respect to height, the density of the delivered volcanic clouds is balanced to the ambient atmospheric density at the upper atmosphere. Then, the volcanic clouds lose the upward momentum, and spread horizontally. In this thesis, the height where the densities of the volcanic clouds and the ambient atmosphere are balanced is called "neutral height". By settling the above arguments, a typical shape of the volcanic clouds with an explosive eruption could be illustrated in Figure 4.1.

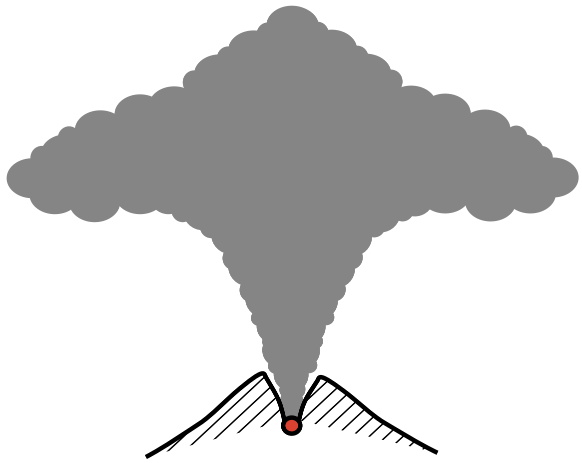

Figure 4.1: Typical shape of the volcanic clouds with an explosive eruption.

To model one of the primary dynamics, i.e., the mixing of the magma and the air, the 2FM is used in the proposed method. The magma and the air are treated in a scheme by using the 2FM, and the mixing is considered. Although, the entrainment assumption that can describe the mixing has an experimental evidence [40], it can be applied to only models of self-similar flow. The self-similar flow is a flow that its radius $r$ is proportion to height $z$ and its velocity $v$ is proportion to exponentiation of height $z$. That is, $r \propto z, v \propto z^k$, where $k$ is a constant. Therefore, the entrainment assumption might be suitable for some models, but unsuitable for models for realistic representation.

## 4.3 Model

This section proposes the model of volcanic clouds with an explosive eruption. In this proposal, to modeling of volcanic clouds, the advection of the magma and the air according to the velocity field is modeled, and the mixing of the magma and the air that is one of the essential factors of the dynamics of volcanic clouds is considered.

### 4.3.1 Evolution of velocity field

The viscosity of the magma due to the intermolecular attractive force of the pyroclasts, and the viscosity of the air are negligible. Moreover, the eruption velocity of the magma is less than the sonic speed. Hence, in this proposed method, the time evolution of the velocity field is defined as the following non-viscosity Navier-Stokes equations.

$$\nabla \cdot \mathbf{u} = 0, \tag{4.1}$$

$$\frac{\partial \mathbf{u}}{\partial t} = -(\mathbf{u} \cdot \nabla)\mathbf{u} - \nabla p + \mathbf{f}, \tag{4.2}$$

where $\mathbf{u}$ is a velocity vector, $p$ is the pressure, and $\mathbf{f}$ is an external force that is applied to the velocity field. These equations are the same as for the modeling method using CML (Equations (3.1) and (3.2) in Subsection 3.2.1), and are described in detail. Hence, the details are omitted here.

### 4.3.2 Evolution of magma and air

The magma and the air are conveyed by the velocity field. Therefore, the following equations can be define for the time evolutions of the magma density $\rho_m$ and the air density $\rho_a$.

$$\frac{\partial \rho_m}{\partial t} = -\left(\mathbf{u} \cdot \nabla\right) \rho_m, \tag{4.3}$$

$$\frac{\partial \rho_a}{\partial t} = -\left(\mathbf{u} \cdot \nabla\right) \rho_a. \tag{4.4}$$

### 4.3.3 Density of the volcanic clouds

The volume of the volcanic clouds per an unit mass $1/\rho_b$ is given by

$$\frac{1}{\rho_b} = \frac{(1-\alpha)(1-n_a)}{\rho_{solid}} + \frac{\alpha(1-n_a)}{\rho_{gas}} + \frac{n_a}{\rho_{gas}}, \tag{4.5}$$

where $\alpha$ is the mass fraction of the volcanic gas in the volcanic clouds, $n_a$ is the mass fraction of the air, $\rho_{solid}$ is the density of the solid part in the volcanic clouds, and $\rho_{gas}$ is the density of the gas part in the volcanic clouds. Here,

$$n_a = \frac{\rho_a}{\rho_m + \rho_a}. \tag{4.6}$$

The first term of the right hand of Equation (4.5) is the volume fraction of the solid part in the volcanic clouds. Since it is less than 1 $vol\%$ in general, the first term is negligible. Thus, Equation (4.5) can be deformed as follows by omitting the first term and using the gas equation.

$$\frac{1}{\rho_b} = \frac{\{\alpha(1-n_a) + n_a\} R_{gas} T_b}{p_{gas}}, \tag{4.7}$$

where $R_{gas}$ is the gas constant of the gas part in the volcanic clouds, $T_b$ is the temperature of the volcanic clouds, $p_{gas}$ is the pressure of the gas part in the volcanic clouds. Then, $R_{gas}$ is given by

$$R_{gas} = \frac{\alpha(1-n_a)R_m + n_a R_a}{\alpha(1-n_a) + n_a}, \tag{4.8}$$

where $R_m$ is the gas constant of the volcanic gas (462 $J/kg \cdot K$), and $R_m$ is the gas constant of the air (287 $J/kg \cdot K$). $T_b$ is given by

$$T_b = \frac{(1-n_a)C_m T_m + n_a C_a T_a}{(1-n_a)C_m + n_a C_a}, \tag{4.9}$$

where $C_m$ is the specific heat at constant pressure of the magma (1847 $J/kg \cdot K$), and $C_a$ the specific heat at constant pressure of the air (1005 $J/kg \cdot K$). Here, Equation (4.7) can be transformed as follows by substituting Equations (4.6) and (4.9), and using the gas equation.

$$\rho_b = \frac{\rho_a R_a T_a}{\alpha(1-n_a)R_m + n_a R_a} \times \frac{(1-n_a)C_m + n_a C_a}{(1-n_a)C_m T_m + n_a C_a T_a}. \tag{4.10}$$

The profiles of the relationship between $\rho_b$ and $n_m$ or $n_a$ are nonlinear. Figure 4.2 illustrates the nonlinear relationship between the volcanic cloud density that is standardized by the air density $\rho_b/\rho_a$ and the mass fraction of the air $n_a$, when $\alpha = 5$ $wt\%$, $T_a = 300$ $K$, and $T_m = 1000$ $K$.

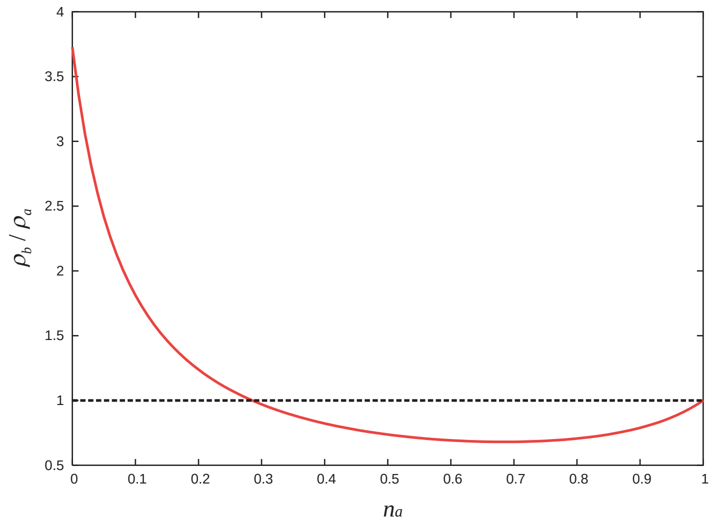


Figure 4.2: The nonlinear relationship between $\rho_b/\rho_a$ and $n_a$, when $\alpha = 5\ wt\%$, $T_a = 300\ K$, and $T_m = 1000\ K$.

When $T_m$ and $T_a$ are constant, $\rho_b$ becomes a function of only $\rho_m$ and $\rho_a$. Note that $n_a = \rho_a/(\rho_m + \rho_a)$ (Equation (4.6)). In the proposed method, the temperatures of the magma and the air are assumed as constants for the following reasons.

- The thermal capacity of the magma is large, that is the temperature of the magma do not change largely. So, it is assumable that the temperature of the magma is a constant.

- The large part of the entrained air to the volcanic clouds is the atmosphere at low hight. Thus, the temperature of the entrained air can be regarded as a constant.

By these assumptions, the look-up table of the relationship between $\rho_b/\rho_a$ and $n_a$ can be made in a preprocessing. Therefore, in the proposed method, since the look-up table is available, the calculation of Equation (4.10) that is a complex equation during the simulation is unneeded. The calculation of Equation (4.10) for all voxels at every time step is clearly consumes huge time, and it should be avoided for the aim of the proposed method.

### 4.3.4 Buoyancy

The buoyancy is occured due to the difference of densities of the volcanic clouds $\rho_b$ and the ambient atmosphere $\rho_{a_{atm}}$. Therefore, the equation for the buoyancy $\mathbf{f}_{buoy}$ can be defined as follows.

$$\mathbf{f}_{buoy} = g\frac{\rho_{a_{atm}}(z) - \rho_b}{\rho_b}\mathbf{z}, \tag{4.11}$$

where $g$ is the gravity constant ($9.8\ m/s^2$), $\mathbf{z}$ is a perpendicularly upward unit vector, and $\rho_{a_{atm}}(z)$ is the atmospheric density. $\rho_{a_{atm}}(z)$ is defined as the following equation.

$$\rho_{a_{atm}}(z) = \rho_0 \exp\left(-\frac{z}{H_e}\right), \tag{4.12}$$

where $\rho_0$ is the density atmosphere at the ground ($z = 0$), and $H_e$ is the scale height where the atmospheric density is $1/e$ (typically, approximately $8\ km$). This equation is the same as Equation (3.6) in Subsection 3.2.3.

### 4.3.5 Fluid solver

The fluid solver for the model using the 2FM is described in this subsection. The fluid solvers for the proposed models are basically the same. And the fluid solver for the propsed model using the CML method is described in Subsection 3.2.4. Therefore, in this subsection, only the unique parts of the solver for the proposed model using the 2FM is described, and the common parts of the solvers for the proposed models are omitted.

#### Setting of analysis space

The analysis space is represented as $n_x \times n_y \times n_z$ cubic voxels with uniform size. At the center of each voxel, the state variables, i.e., the velocity vector $\mathbf{u}$, the magma density $\rho_m$, and the air density $\rho_a$ are defined. For all voxels except the voxels correspond to the mountain and the vent, $\mathbf{u}$ is initialized by small value by using a random function, $\rho_m$ is initialized by zero, and $\rho_a$ at each height are initialized by $\rho_{a_{atm}}(z)$. The boundary conditions for the voxels that correspond to the mountain are $\mathbf{u} = \mathbf{0}$ and $\rho_m = \rho_a = 0$. And the eruption velocity $\mathbf{u}_{src}$, initial magma density $\rho_{b_{src}}$ are assigned to the voxels corresponding to the vent.

### Sequential solver

The volcanic clouds behaviour is obtained by iterating the following processes.

1. **Add force**
   "Add force" is the process to add the external force to the velocity fluid.

2. **Advect**
   "Advect" is the process to advect the state variables.

3. **Project**
   "Project" is the process to vary the velocity with respect to the gradient of the pressure, and project the velocity vector to the divergent free field.

4. **Mix**
   "Mix" is the process to obtain the volcanic cloud density using the look-up table of the relation between $\rho_b/\rho_a$ and $n_a$.

**Add force** The effect of the external force as the third term of the right hand of Equation (4.2) is calculated in Add force process. The external force $\mathbf{f}$ is the sum of the buoyancy $\mathbf{f}_{buoy}$, and the external force of the vorticity confinment $\mathbf{f}_{conf}$. $\mathbf{f}_{conf}$ is force to represent small scale vortexes lost during the simulation, and is given by

$$\mathbf{f}_{conf} = \varepsilon(\mathbf{N} \times \boldsymbol{\omega}), \tag{4.13}$$

$$\boldsymbol{\omega} = \nabla \times \mathbf{u}, \quad \mathbf{N} = \frac{\nabla |\boldsymbol{\omega}|}{|\nabla |\boldsymbol{\omega}||},$$

where $\varepsilon$ is a positive constant and means the degree of the vorticity confinement (see [38] for the details). Moreover, $\varepsilon$ is proportion to the size of the voxel. Hence, the equation for updating the velocity vector $\mathbf{u}$ is expressed as follows.

$$\mathbf{u}^* = \mathbf{u} + (\mathbf{f}_{buoy} + \mathbf{f}_{conf})\Delta t, \tag{4.14}$$

where $\mathbf{u}^*$ is the velocity vector after being updated while a time step $\Delta t$.

**Advect** The effects of the advection as the first term of the right hand of Equation (4.2), (4.3), and (4.4) are calculated in Advect process. By using the semi-Lagrangian advection scheme that is described in Subsection 3.2.4, the equations for updating the state variables are expressed as follows.

$$\mathbf{u}^*(\mathbf{x}) = \mathbf{u}(\mathbf{p}(\mathbf{x}, \Delta t)), \tag{4.15}$$

$$\rho_m^*(\mathbf{x}) = \rho_m(\mathbf{p}(\mathbf{x}, \Delta t)), \tag{4.16}$$

$$\rho_a^*(\mathbf{x}) = \rho_a(\mathbf{p}(\mathbf{x}, \Delta t)), \tag{4.17}$$

where the definition of $\mathbf{p}(\mathbf{x}, \Delta t)$ is the same as in Equations (3.8) and (3.9) that are in Subsection 3.2.4. And $\mathbf{u}^*$, $\rho_m^*$ and $\rho_a^*$ are the velocity vector, the magma density, and the air density after being updated while a time step $\Delta t$, respectively.

**Project** The effect of the continuity constraint as Equation (4.1) and the effect of the pressure as the second term of the right hand of Equation (4.2) is calculated in Project process. For the calculation, at first, the Poisson equation:

$$\nabla^2 p = \frac{1}{\Delta t}\nabla \cdot \mathbf{u} \tag{4.18}$$

should be solved. There are many Poisson solvers. One of the most popular Poisson solvers is the Gaussian elimination. However its complexity is $O(N^3)$, that is, needs a huge calculation time. Therefore, it is unsuitable for the proposed method. To avoid such problem, iterative methods such as the Gauss-Seidel iteration method, the Jacobi's iteration method, and the conjugate gradient (CG) method are useful. In these methods, the CG method is used in this research, since it converges fast and, is easy to implement.

Once the pressure $p$ is obtained by solving Equation (4.18), the equation for updating the velocity vector $\mathbf{u}$ is expressed as follows.

$$\mathbf{u}^* = \mathbf{u} - \nabla p \Delta t, \tag{4.19}$$

where $\mathbf{u}^*$ is the velocity vector after being updated while a time step $\Delta t$.

**Mix** The volcanic cloud density is calculated in Mix process. In the proposed method, it is achieved by only referring the look-up table of the relation between $\rho_b/\rho_a$ and $n_a$ that is described in Subsection 4.3.3.

## 4.4 Result

The images generated by the proposed method are shown in Figures 4.3-4.8. The conditions of the simulations were $\mathbf{u}_{src} = 100\ m/s$, $T_a = 300\ K$, and $\alpha = 5\ wt\%$. $T_m$ was changed from 700 $K$ to 1000 $K$ at 100 $K$ intervals. Figure 4.3 shows the image to show the case when $T_m = 700\ K$. Round and low volcanic clouds were generated, since the temperature of the magma was low. Thus, the volcanic clouds cloud not get enough buoyancy to generate a volcanic column. Figure 4.4 shows the image to show the case when $T_m = 800\ K$. Conic volcanic clouds were generated, since the maximum height of the volcanic clouds was almost the neutral height. Figure 4.5 shows the image to show the case when $T_m = 900\ K$. Mushroom-like volcanic clouds were generated, since the maximum height of the volcanic clouds was beyond the neutral height. Figure 4.6 shows the image to show the case when $T_m = 1000\ K$. The maximum height of the volcanic clouds largely exceeded the neutral height, i.e., the overshoot was occurred, since the temperature of the magma was high. For comparison of the maximum height at each magma temperature, Figure 4.7 shows the images of volcanic clouds from the unique view point. The shapes of the volcanic clouds are same as Figures 4.3-4.6. The Figure 4.8 shows a sequence of images of the volcanic clouds eruption. The final frame is same as Figure 4.6. Figure 4.9 shows a photograph of a real volcanic clouds and the volcanic clouds generated by the proposed method shown in Figure 4.6 for comparision. The shape of clouds' outline of the photograph is similar to the image generated by the proposed method.

The images in Figures 4.3, 4.4, 4.5, and 4.6, are the simulation results on $100 \times 100 \times 75$ voxels, $150 \times 150 \times 100$ voxels, $150 \times 150 \times 150$ voxels, and $100 \times 100 \times 150$ voxels, respectively. The size of voxel was 100 $m^3$. The visualization was done by using the method described in Chapter 5. The computational time of the simulation was approximately 2 second per time step on a Pentium 4 2.8 GHz CPU machine.

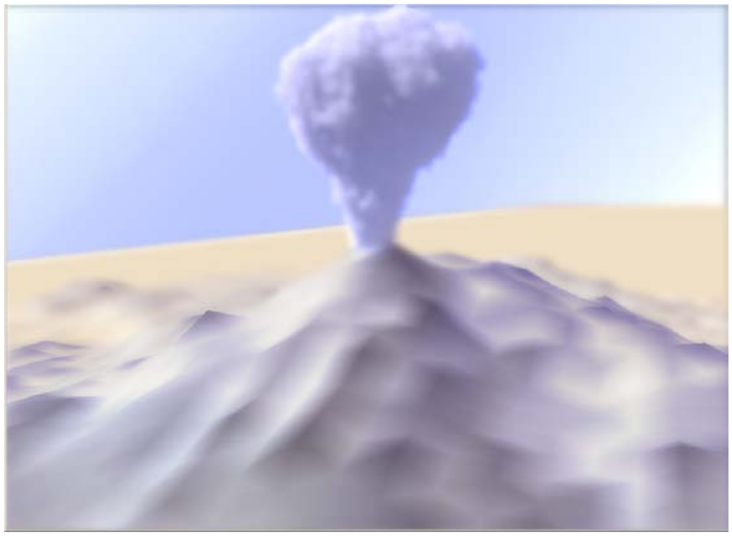

Figure 4.3: Round and low volcanic clouds generated by the proposed method. $T_m = 700\ K$.

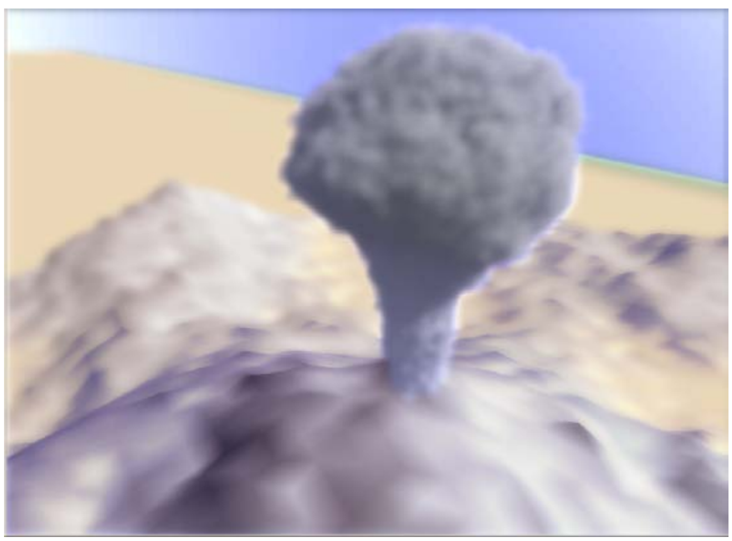

Figure 4.4: Conic volcanic clouds generated by the proposed method. $T_m = 800\ K$.

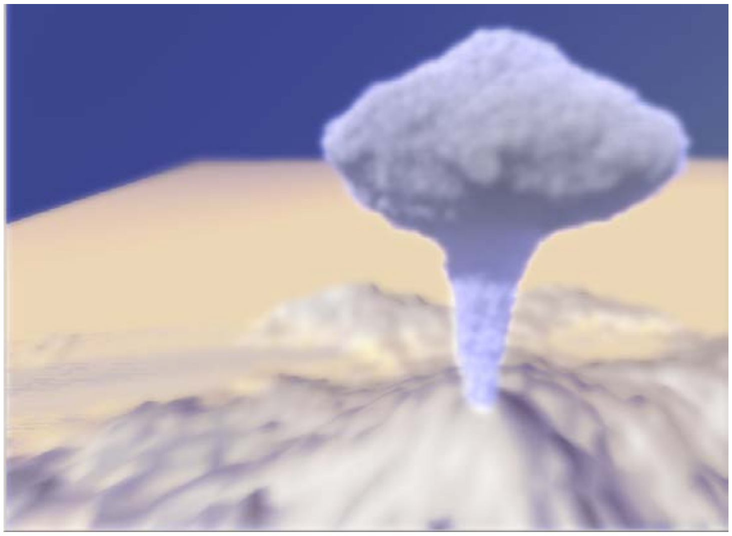

Figure 4.5: Mushroom-like volcanic clouds generated by the proposed method. $T_m = 900\ K$.

Figure 4.6: The overshoot was represented by the proposed method. $T_m = 1000\ K$.

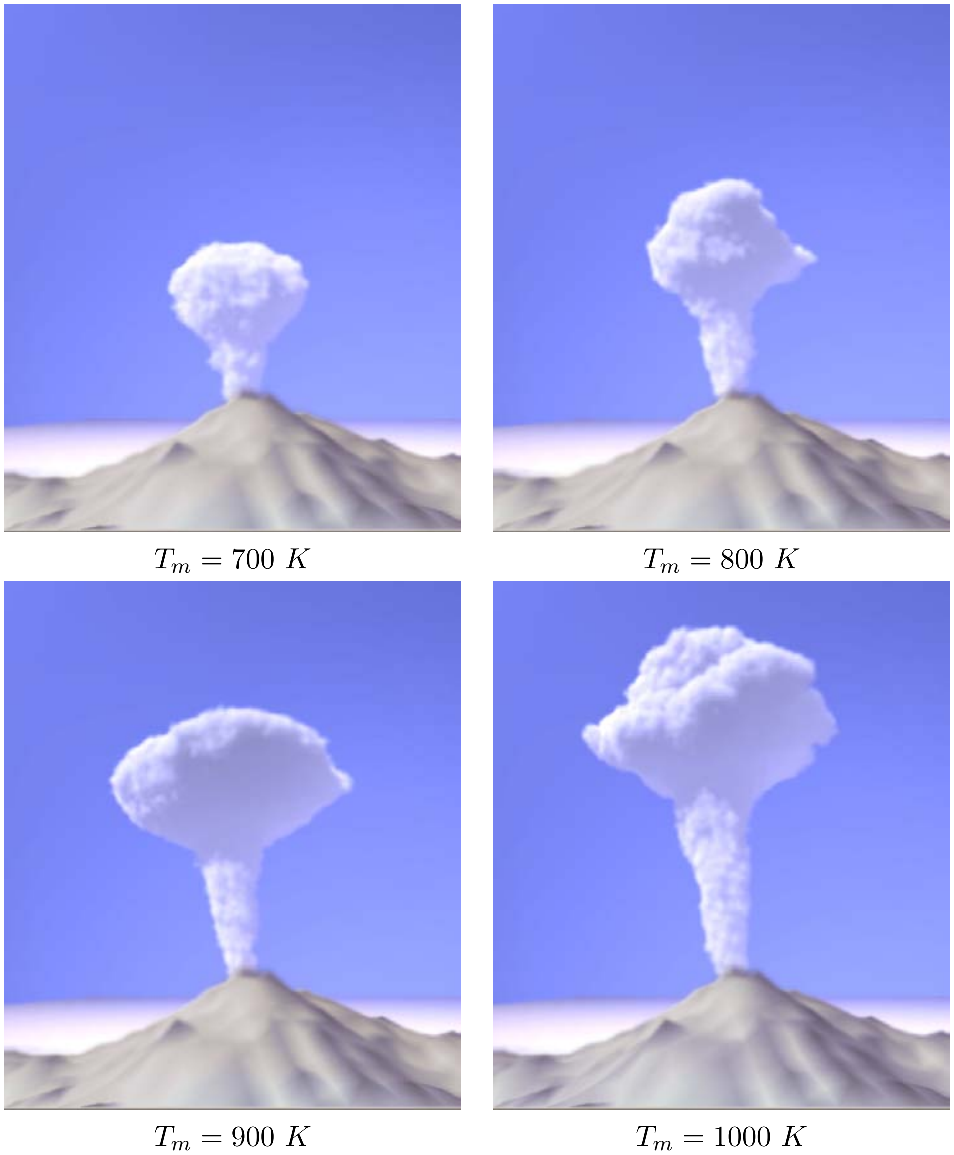

$T_m = 700\ K$ $T_m = 800\ K$

$T_m = 900\ K$ $T_m = 1000\ K$

Figure 4.7: Comparison of the maximum height at each magma temperature.

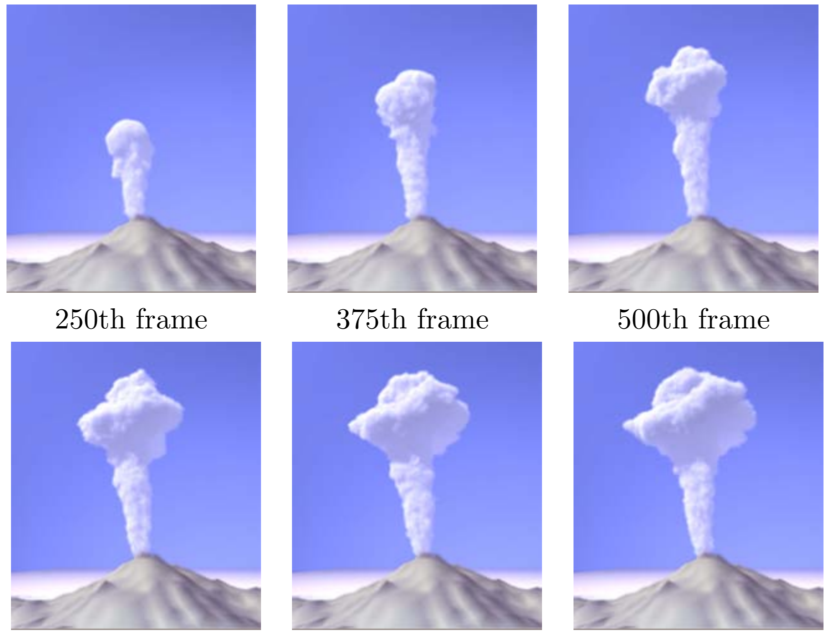

250th frame 375th frame 500th frame

625th frame 750th frame 1000th frame

Figure 4.8: A sequence of images of the volcanic clouds with an explosive eruption. The final frame is same as Figure 4.6.

Figure 4.9: A photograph of real volcanic clouds and the image of the volcanic clouds generated by the proposed method shown in Figure 4.6 for comparision. The copyright of the photograph has been reserved by University of Guelph.

## 4.5 Conclusion and Future Work

In this chapter, a method for the modeling of volcanic clouds using the 2FM was provided. The major features of the proposed method are:

- By the simulation based on the simplified dynamics of volcanic clouds, the realistic and quantitatively reasonable behaviour of volcanic clouds can be represented.

- The quantitative and three dimensional simulation of volcanic clouds behaviour can be done in a practical calculation time.

To enhance the quantitative accuracy of the simulation, the variety of the density with respect to the pressure might be considered. In this case, the equation that describes the time evolution of compressible fluid should be used. A model considering the variety of the density with respect to the pressure is being investigated now.

# Chapter 5

# Visualization of Volcanic Clouds

This chapter describes the visualizing method of the volcanic clouds generated by the proposed modeling methods in Chapters 3 and 4 [5]. This method was originally the visualization method of lightning considering scattering effects due to clouds and atmospheric particles. In this thesis, the method is applied to the visualization of volcanic clouds.

## 5.1 Visualization of Clouds

Figure 5.1 shows the idea of calculating the color of clouds taking into account the single scattering of light. First, the sum of the scattered light reaching from the sun on the viewing ray is calculated. The attenuated light reaching from behind the clouds is also calculated. The light reaching the viewpoint is the sum of those two. Therefore, the color of a voxel depends on the scattered color of the sun, the transmitted color of the sky, and the attenuation due to cloud particles. Calculation of cloud color using splatting [1, 25, 42] is as follows. First, as shown in Figure 5.2, textures for billboards are precalculated. Each element of the texture stores the attenuation ratio and cumulative density of the light passing through the metaball [45] (see Figure 5.2). Since the attenuation is not proportional to it, the texture has to be prepared for all meatballs when their center densities are different. However, this requires a large amount of memory. So, the density is discretized into $n_q$ levels and $n_q$ textures are prepared. The texture corresponding to the nearest density of each metaball is mapped onto the corresponding billboard. An image is calculated in two steps using the texture-mapped billboards. In the first step, the intensity of the light is calculated reaching from the sun at each metaball. The shadows of the clouds are also calculated in this step.

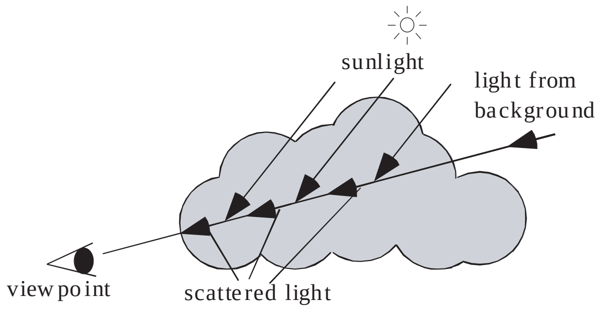


Figure 5.1: Calculation of cloud color.

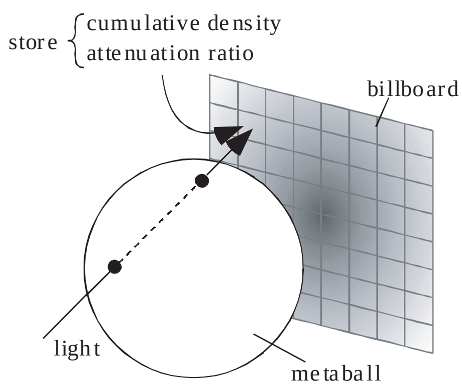


Figure 5.2: Billboard and its texture.

In the second step, the image viewed from the viewpoint is generated. The two steps are as follows. Figure 5.3 shows the idea of the first step. The basic idea is to calculate an image viewed from the sun direction to obtain the intensity of light reaching each metaball. First, the viewpoint is placed at the sun position and the parallel projection is assumed. The frame buffer is initialized as 1.0. Then the billboards are placed at the center of each metaball with their normals oriented to the sun direction as shown in Figure 5.3(a). Next, attenuation ratio between the center of each metaball and the sun is calculated. For example, the attenuation ratio between the metaball C and the sun is obtained by multiplying the attenuation ratio of metaballs A, B, and D (see Figure 5.3(a)). To do this for all metaballs, the billboards are sorted in ascending order using the distance from the sun (the order is B-E-A-D-C in Figure 5.3). Then, beginning from metaball B, they are projected onto the image plane. The values in the frame buffer are multiplied by their attenuation ratios that are stored in the billboard texture (Figure 5.3(b)). This can be easily done by using blending functions of OpenGL [46]. Then the pixel value corresponding to the center of the metaball is read from the frame buffer. The value obtained is the attenuation ratio between the sun and the metaball. The color of the metaball is obtained by multiplying the pixel value by the sunlight color. These processes are repeated for all metaballs. After all the metaballs are processed, the image in the frame buffer stores the attenuation ratio of the sunlight passing through the clouds (Figure 5.3(c)). The image is stored as a light map texture [1] to cast shadows on the ground.

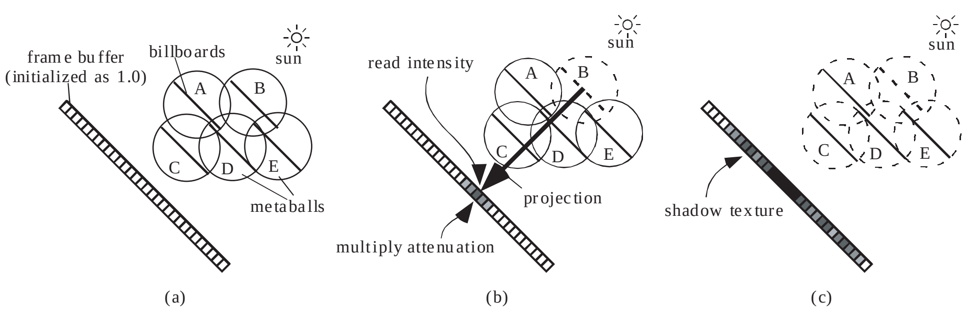


Figure 5.3: Algorithm for calculating the intensity of light reaching the center of metaballs. (a) Billboards are placed at the centers of metaballs and sorted based on their distances from the sun. The frame buffer is initialized as 1.0. (b) Billboards are projected onto the image plane. The colors in the frame buffer are multiplied by attenuation stored in billboard textures. (c) Shadow texture is obtained in the frame buffer. Each element stores the attenuation of light passing through clouds.

In the second step, the image is generated by using the color of the metaball obtained in the first step. First, all the objects except clouds are visualized. Next, as shown in Figure 5.4(a), the billboards are faced perpendicularly to the viewpoint and sorted in descending order based on distances from the viewpoint (the order is E-B-D-A-C). Then they are projected onto the image plane in back-to-front order (Figure 5.4(b)). The color in the frame buffer is blended with that of the billboard texture. The blending process is the same as the one used in the splatting method (see [1] for the details). That is, the colors in the frame buffer are multiplied by the attenuation ratio of the billboard texture and then the colors in the texture are added. The process is repeated for all metaballs.

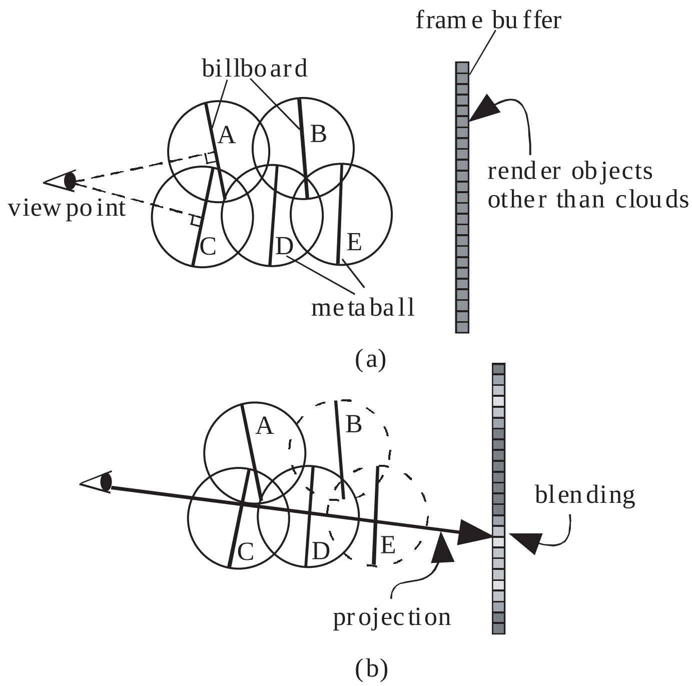


Figure 5.4: Algorithm for generating images. (a) Billboards are oriented to the viewpoint and sorted based on their distances from the viewpoint. (b) Billboards are projected onto the image plane. The colors in the frame buffer are attenuated and blended with the colors in the billboard textures.

# Chapter 6

# Conclusion

This chapter concludes this thesis. This thesis has addressed the modeling method of volcanic clouds for computer graphics. The following two modeling methods have been proposed.

- Chapter 3 has presented the modeling method using the CML method. By using the CML method, the proposed method can represent the realistic behaviour of volcanic clouds in a practical calculation time. Moreover, by this method, the various shapes of volcanic clouds can be generated by changing only several parameters provided in the proposed method. Therefore, this method could be used for entertainments purposes.

- The modeling method using the 2FM has been presented in Chapter 4. This method can represent the realistic and quantitatively reasonable behaviour of volcanic clouds as the result of the simulation based on the simplified dynamics of volcanic clouds. Furthermore, The quantitatively reasonable three dimensional simulation of volcanic clouds behaviour in a practical calculation time has been achieved by the proposed method. Hence, one of the applications of this method is a natural disaster simulation.

Moreover, Chapter 5 has presented the visualization method of the modeling results. However, in addition to addressing the future work described in

Sections 3.4 and 4.5, there is still room for improvement in this research direction. That is, we have to seek the way to the hard goal, which is to establish simple models for complex phenomena.

# Bibliography


[1] D. Blythe, Advanced Graphics Programming Techniques Using OpenGL, *Course Note #29 of SIGGRAPH 99*, 1999.

[2] M. Chen, A. E. Kaufman, and R. Yagel, Voluem Graphics, *Springer*, 215, 2000.

[3] Y. Dobashi, T. Nishita, H. Yamashita, and T. Okita, Using Metaballs to Modeling and Animate Clouds from Satellite Images, *The Visual Computer*, 15(9): 471-482, 1998.

[4] Y. Dobashi, K. Kaneda, H. Yamashita, T. Okita and T. Nishita, A Simple, Efficient Method for Realistic Animation of Clouds, *Proc. SIGGRAPH 2000*, 31-37, 2000.

[5] Y. Dobashi, T. Yamamoto, and T. Nishita, Efficient Rendering of Lightning Taking into Account Scattering Effects due to Clouds and Atmospheric Particles, *Proc. Pacific Graphics 2001*, 390-399, 2001.

[6] F. Dobran, A. Neri, and M. Todesco, Assessing the pyroclastic flow hazard at Vesuvius, *Nature*, 367: 551-554, 1994.

[7] D. S. Ebert and R. E. Parent, Rendering and Animation of Gaseous Phenomena by Combining Fast Volume and Scanline A-Buffer Techniques, *Computer Graphics*, 24(4): 357-366, 1990.

[8] D. P. Enright, S. Marschner, and R. Fedkiw, Animation and Rendering of Complex Water Surfaces, *Transaction on Graphics (Proc. SIGGRAPH 2002)*, 21(3): 736-744, 2002.

[9] R. Fedkiw, J. Stam, and H. W. Jensen, Visual Simulation of Smoke, *Proc. SIGGRAPH 2001*, 15-22, 2001.

[10] N. Foster and D. Metaxas, Realistic Animation of Liquids, *Graphical Models and Image Processing*, 58(5): 471-483, 1996.

[11] N. Foster and D. Metaxas, Modeling the Motion of Hot, Turbulent Gas, *Proc. SIGGRAPH 97*, 181-188, 1997.

[12] N. Foster and R. Fedkiw, Practical Animations of Liquids, *Proc. SIGGRAPH 2001*, 23-30, 2001.

[13] G.Y. Gardner, Visual Simulation of Clouds, *Computer Graphics*, 19(3): 279-303, 1985.

[14] M. J. Harris, G. Coombe, T. Scheuermann, and A. Lastra, Physically-Based Visual Simulation on Graphics Hardware, *Proc. SIGGRAPH / Eurographics Workshop on Graphics Hardware 2002*, 109-118, 2002.

[15] Y. Ishimine and T. Koyaguchi, Numerical Study on Volcanic Eruptions, *Computational Fluid Dynamics Journal*, 8(1): 69-75, 1999.

[16] Y. Ishimine, Numerical study of volcanic eruption columns, *A Doctor Thesis of The University of Tokyo*, 2000.

[17] J. T. Kajiya and B. P. von Herzen, Ray Tracing Volume Densities, *Computer Graphics (Proc. SIGGRAPH 84)*, 18(3): 165-174, 1984.

[18] K. Kaneda, T. Okamoto, E. Nakamae, and T. Nishita, Photorealistic Image Synthesis for Outdoor Scenery under Various Atmospheric Conditions, *The Visual Computer*, 7(5&6): 247-258, 1991.

[19] K. Kaneko, Simulating Physics with Coupled Map Lattices —— Pattern Dynamics, Information Flow, and Thermodynamics of Spatiotemporal Chaos, *Formation, Dynamics, and Statistics of Patterns: World. Sci.*, 1-52, 1990.

[20] K. Kaneko, Coupled Maps: from Local to Global, *Computational Physics as a New Frontier in Condensed Matter Research*, 219-302, 1995.

[21] T. Koyaguchi, Physics of Volcanic Cloud, *Parity*, 15 (11): 30-36, 2000.

[22] A. Lamorlette and N. Foster, Structural Modeling of Natural Flames, *Transaction on Graphics (Proc. SIGGRAPH 2002)*, 21(3): 729-735, 2002.

[23] N. Max, R. Crawfis, and D. Williams, Visualizing Wind Velocities by Advecting Cloud Textures, *Proc. Visualization 92*, 179-183, 1992.

[24] N. Max, Efficient Light Propagation for Multiple Anisotropic Volume Scattering, *Proc. the Fifth Eurographics Workshop on Rendering*, 87-104, 1994.

[25] K. Meuller, N. Shareef, J. Huang, and R. Crawfis, High-Quality Splatting on Rectilinear Grids with Efficient Culling of Occluded Voxels, *IEEE Trans. on Visualization and Computer Graphics*, 5(2): 116-134, 1999.

[26] R. Miyazaki, S. Yoshida, Y. Dobashi, and T. Nishita, A Method for Modeling Clouds based on Atmospheric Fluid Dynamics, *Proc. Pacific Graphics 2001*, 363-372, 2001.

[27] R. Mizuno, Y. Dobashi, and T. Nishita, Simulation and Visualization of Volcanic Smoke using CML, *Proc. IPSJ 64th Zenkoku-Taikai*, 4: 737-738, 2002.

[28] R. Mizuno, Y. Dobashi, and T. Nishita, Animation of Volcanic Smoke using CML, *Proc. IPSJ 108th CG&CAD Summer Meeting*, 115-120, 2002.

[29] R. Mizuno, Y. Dobashi, and T. Nishita, Volcanic Smoke Animation using CML, *Proc. International Computer Symposium 2002*, 2: 1375-1382, 2002.

[30] R. Mizuno, Y. Dobashi, and T. Nishita, Simulation and Visualization of Volcanic Cloud using 2 Fluids Model, *Proc. IPSJ 65th Zenkoku-Taikai*, (be appear), 2003.

[31] A. Neri and G. Macedonio, Numerical simulation of collapsing volcanic columns with particles of two sizes, *Journal of Geophysical Research*, 101(B4): 8153-8174, 1996.

[32] D. Nguyen, R. Fedkiw, and H. W. Jensen, Physically Based Modeling and Animation of Fire, *Transaction on Graphics (Proc. SIGGRAPH 2002)*, 21(3): 721-728, 2002.

[33] T. Nishita, Y. Dobashi, and E. Nakamae, Display of Clouds Taking into Account Multiple Anisotropic Scattering and Sky Light, *Proc. SIGGRAPH 96*, 379-386, 1996.

[34] G. Sakas and M. Gerth, Sampling and Anti-Aliasing of Discrete 3-D Volume Density Textures, *Proc. Eurographics 91*, 87-102, 1991.

[35] J. Stam and E. Fiume, Turbulent Wind Fields for Gaseous Phenomena, *Proc. SIGGRAPH 93*, 369-376 1993.

[36] J. Stam and E. Fiume, Dipicting Fire and Other Gaseous Phenomena Using Diffusion Processes, *Proc. SIGGRAPH 95*, 129-136, 1995.

[37] J. Stam, Stable Fluids, *Proc. SIGGRAPH 99*, 121-128, 1999.

[38] J. Steinhoff and D. Underhill, Modification of the euler equations for “ vorticity confinement ”: Application to the computation of interacting vortex rings, *Physics of Fluids*, 6(8): 2738-2744, 1994.

[39] Y. Suzuki, Numerical Simulation of Volcanic Explosive Eruption, *A Master Thesis of The University of Tokyo*, 2001.

[40] J. S. Turner, Turbulent entrainment: the development of the entrainment assumption, and its application to geophysical flows, *Journal of Fluid Mech.*, 173:431-471, 1986.

[41] G. A. Valentine and K. H. Wohletz, Numerical models of Plinian eruption columns and pyroclastic flows, *Journal of Geophysical Research*, 94: 1867-1887, 1989.

[42] L. Westover, Footprint Evaluation for Volume Rendering, *Computer Graphics*, 24(4): 367-376, 1990.

[43] A. W. Woods, The fluid dynamics and thermodynamics of eruption columns, *Bull. Volcanol.*, 50: 169-193, 1988.

[44] A. W. Woods, S. M. Bower, The decompression of volcanic jets in a crater during explosive volcanic eruptions, *Earth and Planetary Science Lett.*, 131: 189-205, 1995.

[45] G. Wyvill and A. Trotman, Ray-Tracing Soft Objects, *Proc. CG International*, 439-475, 1990.

[46] M. Woo, J. Neider, T. Davis, and D. Shreiner, OpenGL Programming Guide Third Edition, *ADDISON-WESLEY*, 2-5, 1999.

[47] T. Yanagita, Coupled Map Lattice Model for Boiling, *Phys. Lett. A*, 165: 405-408, 1992.

[48] T. Yanagita, Phenomenology for Boiling: A Coupled Map Lattice Model, *Chaos*, 3(2): 343, 1992.

[49] T. Yanagita and K. Kaneko, Coupled Map Lattice Model for Convection, *Phys. Lett. A*, 175: 415-420, 1993.

[50] T. Yanagita and K. Kaneko, Rayleigh-Bénard convection: Patterns, chaos, spatiotemporal chaos and turbulence, *Physica D*, 82: 288-313, 1995.

[51] T. Yanagita and K. Kaneko, Modeling and Characterization of Clouds Dynamics, *Phys. Rev. Lett.*, 78(22): 4297-4300, 1997.

[52] G. Yngve, J. O' Brien, and J. Hodgins, Animating Explosions, *Proc. SIGGRAPH 2000*, 29-36, 2000.

[53] Using MAYA: Dynamics (user's manual), 219-224, *Alias|wavefront*, 1999.